Investigating Sub-bandgap Spectral Effects in GaInP-on-Ge Solar Cells

Brianna Conrad and Behrang H. Hamadani
National Institute of Standards and Technology (NIST), Gaithersburg, MD 20899, USA

***Abstract*—There is a fundamental understanding in photovoltaics that sub-bandgap light will not be absorbed in the solar cell and therefore will not affect the power generation. We have shown a novel phenomenon in which sub-bandgap illumination is required for good electrical performance in III-V solar cells on heterosubstrates. We investigate this effect in GaInP cells on Ge substrates with current-voltage measurements under varying spectra and irradiances. This has implications for device characterization, the development of solar cells both on heterosubstrates and for conditions lacking long-wavelength light, and the prediction of device performance under spectra that differ from the test conditions.**

***Index Terms*—III-V and Concentrator PV, Characterization of PV, Circuit analysis, Photovoltaic cells**

I. Introduction

With increased interest in indoor photovoltaics that utilize ambient light to run low-power devices, including sensors for the Internet of Things [1], the operation and characterization of devices at low power densities (i.e., <0.5 W/m^2) and under a variety of spectra, many of which are significantly different from the AM1.5G or AM0 standards [2] is of great importance. As a result, there is a demand for accurate measurements with one test spectrum that can predict device performance under a potentially very different spectrum. Therefore, establishing equivalency between different conditions is essential.

It is common practice to consider only light above the bandgap as contributing significantly to a solar cell's power generation. Measurements are taken with reference cells and calibration is dependent on the product of the test illumination spectra and the spectral responsivities of reference and test cells [3], [4]. Light of wavelengths where the spectral responsivity is negligible is considered superfluous and irrelevant to the power output of the solar cell (aside from any influence on cell temperature). The irradiance level and a reference spectrum (such as AM1.5G) are specified, but the test spectrum is not precisely defined.

We have reported on a phenomenon in which III-V solar cells on heterosubstrates, particularly GaAs cells on Ge substrates, require illumination of the substrate to avoid a reduced fill factor and power output. This means that devices will show different results when measured under different spectra, even if the resulting short circuit currents are the same [5]. In this work, we investigate that effect in GaInP cells on Ge substrates, with a comparison to devices on III-V substrates, and demonstrate that the model we have developed reproduces current-voltage measurements on these cells. We also show that alternate models, including that of a tandem solar cell, cannot reproduce or explain the measurements, and, enabled by the wide bandgap of GaInP, explore the effect that Ge substrate illumination has on dark current-voltage characteristics of these devices.

II. Methods

We obtained commercial GaInP n-on-p, front-and-rear contacted solar cells grown by metal-organic chemical vapor deposition (MOCVD) on germanium substrates from Cesi S.p.A., diced into 2 cm squares and packaged, with a 1-sun efficiency of 15.6 % [6]. We also obtained a 1 cm^2 GaInP solar cell on a III-V substrate from a collaborator. We characterized the devices using current-voltage (IV), spectral responsivity (SR), and absolute electroluminescence (EL) measurements.

We performed IV measurements using a calibrated silicon reference cell and a lab-built multi-zone simulator, with a Xenon lamp and 8 light emitting diodes (LEDs) coupled into a tapered glass waveguide with an output area sufficient to completely and uniformly illuminate the cells. The LEDs in the simulator can each be controlled individually and the broadband cool white LED, 460 nm LED (absorbed entirely in GaInP), and 940 nm LED (transmitted entirely to Ge substrate) were used to selectively illuminate layers of these devices. We measured IV curves under 460 nm LED illumination intensities of 1.3 W/m^2 to 550 W/m^2, with and without additional 940 nm illumination. We measured the irradiance and spectrum of the incident light directly with an in-house calibrated UV-VIS-NIR spectroradiometer.

We also measured absolute EL of the devices with a hyperspectral imaging system and calculated the external radiative efficiency (y_{ext}) as described in detail in [6]. With this, we calculated the photon flux into the Ge substrate, Φ_{Ge}, due to luminescence of the GaInP junction, as a function of that junction's current, I_j, as:

$$\Phi_{Ge} = \frac{y_{ext} n^2 I_j}{qA} \tag{1}$$

where n is the refractive index of GaInP at 680 nm, A is the device area, and q is the elementary charge [7]. SR measurements were performed under a steady state bias light.

Certain commercial equipment, instruments, software, or materials are identified in this paper to specify the experimental procedure adequately. Such identification is not intended to imply recommendation or endorsement by the National Institute of Standards and Technology nor is it intended to imply that the materials or equipment identified is necessarily the best available for the purpose.

III. Results and Discussion

When we measured GaInP devices on Ge substrates under 460 nm LED illumination, we saw a fill factor that was significantly reduced from those same devices measured under either white LED illumination, or a combined 460 nm and 940 nm LED illumination. This is true across a wide range of illumination intensities and can be seen in Fig. 1, in which we plot fill factor and open circuit voltage (Voc) under 460 nm LED illumination, with and without the addition of infrared (IR) illumination from the 940 nm LED. This plot shows that Voc was not affected by the spectrum change. Devices with a III-V substrate saw no difference in either fill factor or Voc as a function of sub-bandgap illumination, as would be expected of most photovoltaic cells.

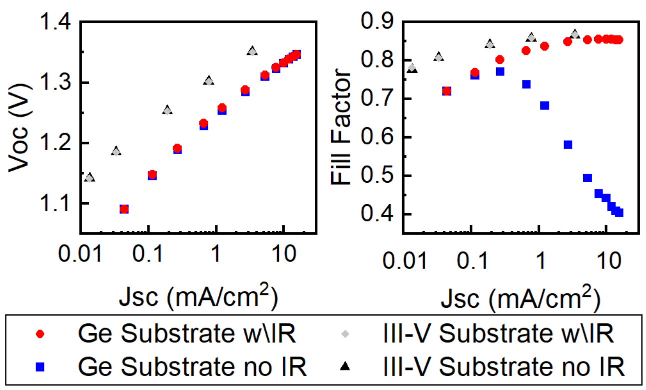

Fig. 1. Short circuit current density dependence of Voc and fill factor of GaInP devices on Ge and III-V substrates with and without 940 nm IR illumination. 940 nm illumination levels are set such that additional 940 nm illumination does not change the Voc and fill factor.

The key difference between these illumination conditions is that the white and 940 nm LED spectra contain wavelengths which pass through the GaInP layers and are absorbed in the Ge substrate. As no portion of the 940 nm LED illumination is absorbed in the active GaInP layers, we can show that when the 460 nm LED irradiance is held constant, the addition of 940 nm illumination will gradually improve the device's current density-voltage (JV) characteristic and fill factor, while having no perceivable effect on the short circuit current (Fig. 2). This allows us to easily measure devices at what would be considered equivalent conditions under the reference cell measurement method, while independently adjusting the sub-bandgap irradiance (i.e., irradiance in the region with negligible spectral response).

In contrast to GaAs cells previously studied in depth [5], the lack of any overlap between the cell's spectral response and the 940 nm LED spectrum also allows us to measure dark JV curves with different substrate illumination conditions by applying only the 940 nm LED. These measurements are shown in Fig. 3. With the reversed direction of current flow, the terminal voltage is increased when there is no substrate illumination, and decreases with added substrate illumination. A minimum is reached at a similar substrate illumination level as that which eliminates the voltage loss in light JV measurements.

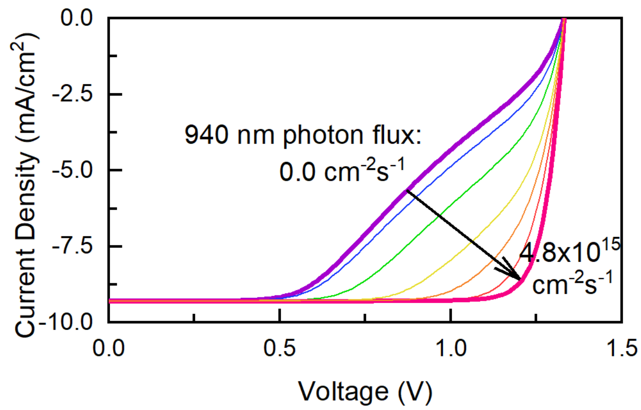

Fig. 2. Effect of progressively higher irradiance from 940 nm LED on the JV curve of a GaInP on Ge cell measured at a fixed 312 W/m^2 460 nm LED irradiance.

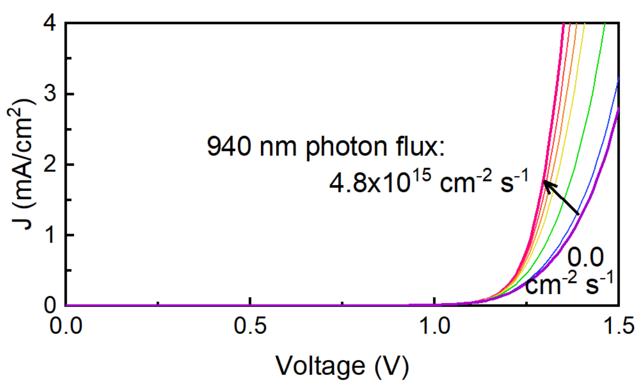

Fig. 3. Dark JV curves of GaInP on Ge device with varying amounts of 940 nm illumination of the Ge substrate.

Fig. 4a shows JV curves with and without 940 nm illumination at several different 460 nm irradiances. For the former case, the irradiance from the 940 nm LED is sufficient that no further improvement is seen if it is increased (i.e. the right-most red curve in Fig. 2). Fig. 4 also shows that if only very low irradiances are considered this effect might be mistaken for a high ohmic series resistance. We also plot the JV curve of devices on III-V substrates, for which no visible distinction can be made between curves measured with and without 940 nm illumination. Differences in short circuit current density (Jsc) and Voc between these devices and those on Ge substrates are not meaningful, as device layouts, optical treatments, and fabrication processes differ.

To explain the device I-V characteristics and reduced fill factor in the absence of IR light, we tested models of a resistance-limited exponential shunt, such as might be present at device edges [8], [9], and of a tandem device with a heavily shunted Ge heterojunction [10], [11] as the bottom junction. Circuit diagrams illustrating these models are seen in Fig. 5, and JV curves derived from them are shown in the gray and

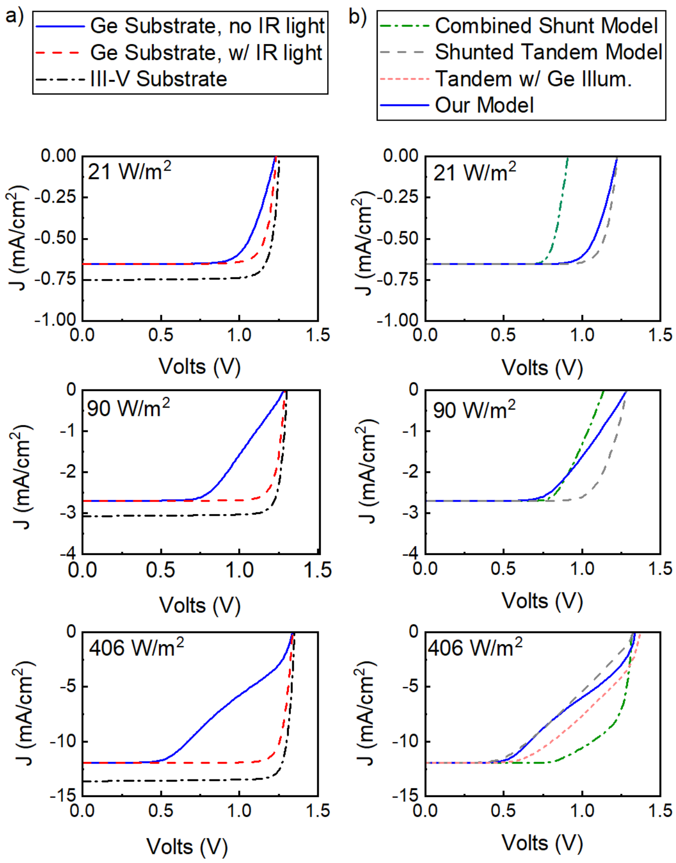

Fig. 4. a) Measured JV curves of GaInP cells on Ge substrates with three different listed levels of 460 nm LED illumination and additional 940 nm LED IR illumination, as well as those of GaInP cells on III-V substrates, for which no distinction is seen between the two illumination conditions. b) JV curves modeled for the same light-generated currents as the Ge-substrate cells using the resistance-limited exponential shunt model, a tandem device model with a significantly shunted bottom junction and reverse breakdown, and the model developed in our work. At 406 W/m^2 we also plot the JV curve with the tandem model under the level of Ge substrate illumination which fully repaired the measured JV curve (red dashed line in part a of this figure).

green broken lines in Fig. 4b. A low reverse breakdown voltage is included for the diode D_B in the tandem model. Although they can each reproduce the measured JV characteristics at some irradiances, neither provides a good explanation over the whole range. For example, the shunt model results in a greatly reduced Voc at low illumination intensities, which is not observed in our measurements. The wide range of irradiance dependent measurements is important therefore in correctly identifying this effect.

As additional evidence to eliminate a tandem device model, we consider the relative illumination level needed to fully repair the JV curve. The fully repaired curve in Fig. 2 was measured with a photon flux of 4.8 x 10^{15} cm^{-2}s^{-1} incident from the 940 nm LED. Luminescence from the GaInP junction near the maximum power point is comparatively negligible. If we were to assume a 100 % internal quantum efficiency (IQE) of a theoretical bottom subcell, this would result in a light-generated current of 0.77 mA/cm^2. This is only 8 % of the 9.3 mA/cm^2 Jsc measured under these conditions, and therefore far short of the illumination that would be required to current match a bottom subcell to the GaInP junction. Fig. 4b also includes, for 406 W/m^2 blue illumination, the JV curve generated by the tandem model with a bottom cell light generated current ($I_{L,B}$ in Fig. 5) equal to that produced by the 940 nm LED illumination which was observed to repair the JV curve, assuming 100 % bottom cell IQE. Not only is the JV curve not repaired, the Voc is increased, which is not observed in measurements.

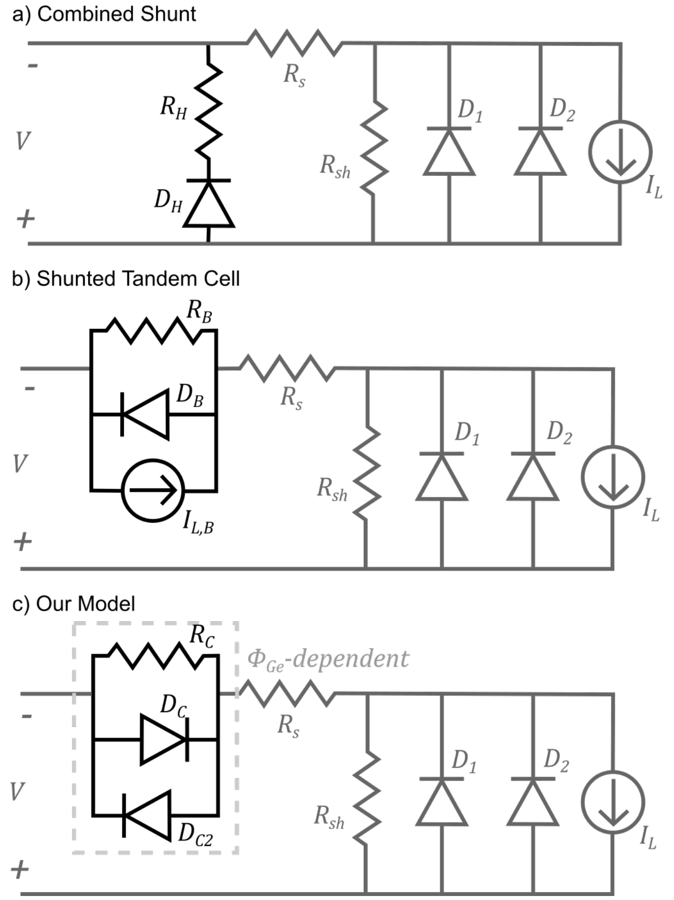

Fig. 5. Circuit diagrams showing: a) solar cell with a resistance-limited exponential shunt, b) tandem solar cell with shunted bottom junction, and c) the model we developed for the GaInP on Ge cells studied in this work.

The dark JV curves shown in Fig. 3 are also inconsistent with a tandem device model. In a tandem device, if we consider a fixed extracted current and illuminate only the bottom junction, $I_{L,B}$ will flow through the bottom junction (D_B in Fig. 5), increasing the total current through that diode, and therefore the voltage across both it and the device terminals. However, in Fig. 3 we see the opposite trend - as the intensity of the 940 nm illumination is increased, the voltage at a fixed extracted current actually decreases. The change in device behavior with long-wavelength illumination is therefore not the result of photogenerated current in the bottom junction of a tandem cell.

We developed the model shown in Fig. 5c to represent the behaviour of these devices. To begin, we find the voltage drop across the loss element, V_C, at different values of extracted device current, I_{ext}, without the influence of Ge substrate illumination. We choose a small fixed value of diode current ($I_L - I_{ext}$), and therefore luminescence, and extract the current and voltage loss at that point for each in a series of measurements at different 460 nm LED irradiances, including the solid blue curves in Fig. 4a. These points are plotted in the first quadrant in Fig. 6 and are well fit by

$$J_t = J_{0,C}(exp(\frac{qV_C}{n_C kT}) - 1) + \frac{V_C}{R_C} \quad (2)$$

which represents the current-voltage characteristic of the diode D_C and resistor R_C in parallel seen in Fig. 5c, with $J_{0,C}$ and n_C being the saturation current density and ideality factor of diode D_C. q is the elementary charge, k is the Boltzmann constant, and T is the device temperature, which we have controlled at 25 °C.

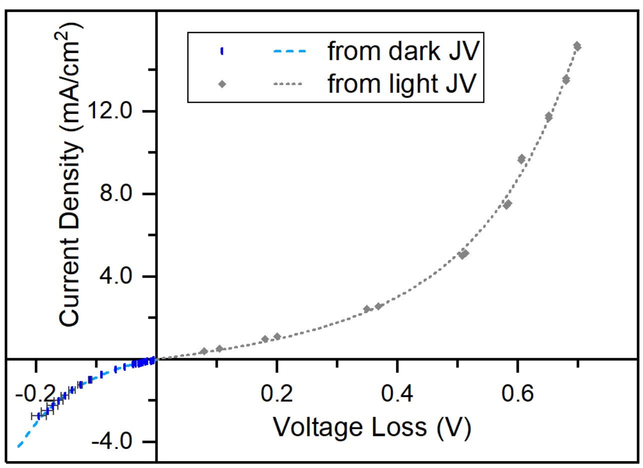

Fig. 6. Voltage loss compared to the condition with high Ge illumination, calculated from both light and dark JV curves.

For the GaInP cells, we are also able to plot the JV characteristics of this element when current is flowing through it in the opposite direction by considering the dark JV curves. Here we take the difference between the curve measured with no 940 nm illumination (rightmost, purple curve in Fig. 3) and the fully repaired curve (leftmost, red curve in Fig. 3), which is not improved with the addition of further 940 nm illumination. As there is still luminescence from the GaInP junction present in this configuration, we estimate an error based on the reduction in voltage loss measured with a small amount of 940 nm illumination. The resulting curve is plotted in the third quadrant in Fig. 6. Even with the uncertainty, a clear exponential characteristic is seen, with the combined linear and exponential characteristic also providing a good fit in this direction. We therefore add diode D_{C2} to the model shown in Fig. 5c. Diodes D_C and D_{C2} are pictured as two separate (ideal) diodes in the circuit model abstraction, but represent one junction with non-ideal characteristics.

To fully model these devices we need to consider in more detail the influence of Ge substrate illumination on the JV characteristics. We have seen that voltage loss is reduced with increasing Ge illumination, so we apply a Ge illumination-dependent modulation to the value of V_C calculated with standard circuit analysis methods (i.e., that which fulfills Eqn. 2). This is a useful approach as it parameterizes the diode and resistor values as a function of the Ge illumination, rather than requiring them to be fit independently at each point in the JV curve. The circuit elements affected by this modulation are outlined in Fig. 5c. For each curve in Fig. 2 we considered the difference between its voltage (V_{ext}) and that of the right-most, fully repaired, curve ($V_{repaired}$) at a fixed I_{ext} as

$$V_C(I_{ext}) = V_{repaired}(I_{ext}) - V_{ext}(I_{ext}) \quad (3)$$

We did the same for I_{ext} in the opposite direction, using the curves shown in Fig. 3. Both are plotted in Fig. 7, with both the measured 940 nm LED illumination and luminescence from the GaInP junction calculated with Eqn. 1 included in the photon flux into the Ge substrate. Fill factor for the light JV curves in Fig. 2 is plotted and shown to increase as the voltage loss decreases. The equivalent current density generated by the illumination in the Ge substrate under a 100 % IQE condition is also shown for simple comparison to the extracted current density.

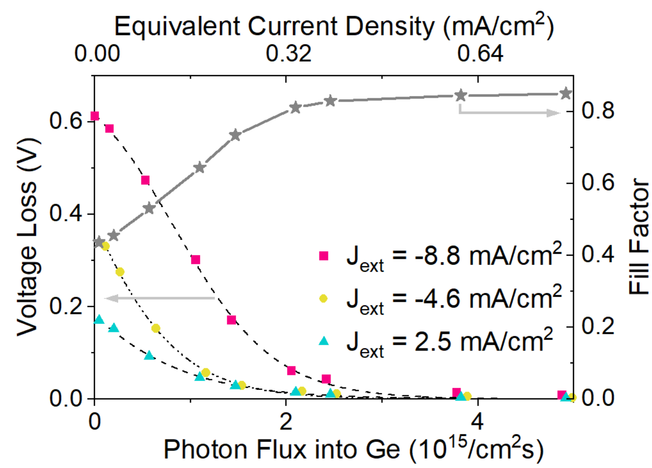

Fig. 7. Voltage loss at several values of fixed extracted current density (J_{ext}) as a function of Ge substrate illumination, with logistic fits to the data. The top axis shows the current which could be generated by the Ge substrate illumination, assuming a 100 % IQE. Fill factor for curves in Fig.2 is also shown.

The voltage loss in both directions is fit to a logistic function:

$$V_C(\Phi_{Ge}) = V_C(dark)\frac{1}{1 + e^{(M - qA\Phi_{Ge})/s}} \quad (4)$$

where M and s are fitting parameters and Φ_{Ge} is the total photon flux into the Ge substrate.

JV curves generated with our model in a mathematical computing environment, including the modulation of V_C with Φ_{Ge} expressed in Eqn. 4 are plotted as solid blue lines

TABLE I
VALUES USED IN VISUAL FITS SHOW IN IN FIG. 7.

Parameter	Value
I_L 21 W/m^2	2.7 mA
I_L 90 W/m^2	10.8 mA
I_L 406 W/m^2	47.8 mA
$I_{0,1}$	6 x10^{-22} mA
$I_{0,2}$	1 x10^{-10} mA
$I_{0,c}$	.008 mA
n_C	3
R_C	40 Ω
R_s	0.3 Ω
M	0.13
s	.064

in Fig. 4b, and reproduce the measured JV characteristics over a range of illumination intensities. The input parameters are varied to visually fit the measured data as shown in Fig. 8. Only the light-generated current I_L is changed between illumination levels, and the values used to produce these fits are listed in Table I. Values of D_{C2} are not included, as they have no significant impact on the light JV characteristics in this quadrent.

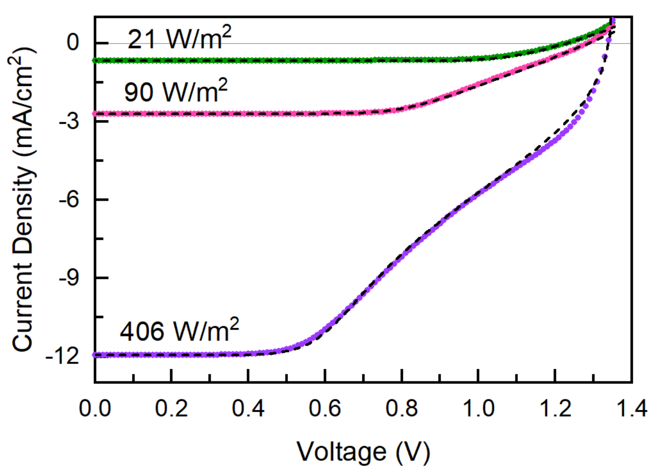

Fig. 8. Visual fit of our model to JV curves measured under varying 460 nm LED irradiances. Parameters for all three irradiances (other than I_L) are the same, and are shown in Table I.

Although our model is similar to that of the tandem cell shown in Fig. 5b, differences arise in the role of long wavelength illumination. In a tandem device, long wavelength illumination generates a photocurrent, while in our model it directly changes the circuit element parameters. The model we developed suggests a barrier to current extraction – likely at the interface between the GaInP and Ge substrate, or between the Ge substrate and a GaAs buffer layer which may be used in MOCVD growth of GaInP on Ge [12]. We found no significant difference between long-wavelength illumination with a 940 nm LED and with a 750 nm LED, which suggests that if any such GaAs layer is present, it is thin enough to not significantly impact transmission to the Ge substrate, and justifies our treatment of photons from the 940 nm LED and the GaInP luminescence around 680 nm as equivalent. Furthermore, the exponential characteristic in both directions is reminiscent of Anderson's model of p-n heterojunctions [13] and characteristics observed in some isotype (n-n or p-p) heterojunctions [14]. Although this barrier is likely formed by a heterojunction, the illumination of the Ge substrate does not affect the overall device JV characteristics through generation of photocurrent as it would in a standard tandem solar cell. Here, the illumination of the Ge substrate likely serves to either adjust the band bending such that the barrier height is reduced, or alter the occupancy of traps near the interfaces to increase lossless tunneling currents.

IV. CONCLUSIONS

Unusual IV characteristics of GaInP on Ge solar cells measured under short wavelength light cannot be explained by edge-shunting or an inadvertent tandem cell. They are well represented by a shunted diode in series the GaInP junction, whose influence is decreased with long-wavelength illumination. This suggests the presence of energy barriers that allow some degree of thermionic emission or tunneling current, which is increased by illumination of the Ge substrate. Ongoing work with temperature-dependent IV measurements will shed more light on the nature of these barriers.

Aside from the specific physical phenomena causing it, these observations are important in informing the way devices are measured and potentially developed. Measurements which appear correctly calibrated on the basis of device short circuit current may not represent device performance under light sources whose sub-bandgap characteristics do not match those of the test source. We have also shown that unusual behavior may not be readily identified from a single measurement - for example this effect appears as high series resistance if only a low-illumination level blue light measurement is considered. We anticipate this will be most relevant for III-V devices grown on Ge or other heterosubstrates, and could be an important phenomenon to be aware of when developing devices using new materials, particularly if also prepared on heterosubstrates. This could be especially relevant to the development of upper subcells for eventual incorporation into multijunction devices, a process which often starts with the development of single-junction cells on inactive heterosubstrates.

ACKNOWLEDGMENT

The authors would like to thank D. T. Bilir, formerly of Solar Junction, for providing the isotype GaInP solar cells on III-V substrates used in this study and for useful discussions.

REFERENCES

[1] I. Mathews, S. N. Kantareddy, T. Buonassisi, and I. M. Peters, "Technology and market perspective for indoor photovoltaic cells," *Joule*, vol. 3, no. 6, pp. 1415 – 1426, 2019.

[2] *G173-03(2020) Standard Tables for Reference Solar Spectral Irradiances: Direct Normal and Hemispherical on 37 Tilted Surface.* West Conshohocken, PA: ASTM International, 2020.

[3] K. Emery and C. Osterwald, "Measurement of photovoltaic device current as a function of voltage, temperature, intensity and spectrum," *Solar Cells*, vol. 21, no. 1, pp. 313 – 327, 1987.

[4] B. H. Hamadani and M. B. Campanelli, “Photovoltaic characterization under artificial low irradiance conditions using reference solar cells,” *IEEE Journal of Photovoltaics*, vol. 10, no. 4, pp. 1119–1125, 2020.

[5] B. Conrad and B. Hamadani, “Sub-bandgap spectral effects in III-V solar cells on heterosubstrates,” *In Review*.

[6] B. H. Hamadani, “Understanding photovoltaic energy losses under indoor lighting conditions,” *Applied Physics Letters*, vol. 117, no. 4, p. 043904, 2020.

[7] S. Chen, L. Zhu, M. Yoshita, T. Mochizuiki, C. Kim, H. Akiyama, M. Imaizumi, and Y. Kanemitsu, “Thorough subcells diagnosis in a multi-junction solar cell via absolute electroluminescence-efficeiency measurements,” *Scientific Reports*, vol. 5, p. 7836, 2015.

[8] K. McIntosh and C. Honsberg, “The influence of edge recombination on a solar cell’s IV curve,” in *16th European Photovoltaic Solar Energy Conference*, 01 2000.

[9] K. Rühle, M. K. Juhl, M. D. Abbott, and M. Kasemann, “Evaluating crystalline silicon solar cells at low light intensities using intensity-dependent analysis of I–V parameters,” *IEEE Journal of Photovoltaics*, vol. 5, no. 3, pp. 926–931, 2015.

[10] J. N. Bullock, C. H. Wu, and J. F. Wise, “Interface contribution to GaAs/Ge heterojunction solar cell efficiency,” *IEEE Transactions on Electron Devices*, vol. 36, no. 7, pp. 1238–1243, 1989.

[11] R. Campesato and C. Flores, “Effects of low temperatures and intensities on GaAs and GaAs/Ge solar cells,” *IEEE Transactions on Electron Devices*, vol. 38, no. 6, pp. 1233–1237, 1991.

[12] T. W. Kim, B. R. Albert, L. C. Kimerling, and J. Michel, “InGaP solar cell on ge-on-si virtual substrate for novel solar power conversion,” *Journal of Applied Physics*, vol. 123, no. 8, p. 085111, 2018.

[13] R. Anderson, “Experiments on Ge-GaAs heterojunctions,” *Solid-State Electronics*, vol. 5, no. 5, pp. 341–351, 1962.

[14] K. Yang, J. R. East, and G. I. Haddad, “Numerical modeling of abrupt heterojunctions using a thermionic-field emission boundary condition,” *Solid-State Electronics*, vol. 36, no. 3, pp. 321–330, 1993.